PHYSICAL REVIEW A **72**, 051601(R) (2005)

Interference of a variable number of coherent atomic sources

Giovanni Cennini, Carsten Geckeler, Gunnar Ritt, and Martin Weitz
Physikalisches Institut der Universität Tübingen, Auf der Morgenstelle 14, 72076 Tübingen, Germany
(Received 2 May 2005; published 1 November 2005)

We have studied the interference of a variable number of independently created $m_F=0$ microcondensates in a CO_2-laser optical lattice. The observed average interference contrast decreases with condensate number N. Our experimental results agree well with the predictions of a random walk model. While the exact result can be given in terms of Kluyver's formula, for a large number of sources a $1/\sqrt{N}$ scaling of the average fringe contrast is obtained. This scaling law is found to be of more general applicability when quantifying the decay of coherence of an ensemble with N independently phased sources.

DOI: 10.1103/PhysRevA.72.051601 PACS number(s): 03.75.Lm, 05.40.Fb, 32.80.Pj, 42.50.Vk

Interference experiments are valuable tools for the study of coherence of atomic sources [1,2]. While for an incoherent ensemble the number of independently phased objects equals the atom number, in a Bose-Einstein condensate atoms macroscopically populate a one-particle quantum state and the whole condensate is a single coherent atom source. Of large interest is the intermediate region of partial coherence. We shall here be interested in the degree of coherence of an ensemble of N-independent quantum objects. For an array of periodically spaced atom sources, each of which is coherent, Ashhab predicted a $1/\sqrt{N}$ scaling of the average fringe visibility with the number of sources N in a far-field interference experiment [3]. For other theoretical works, see [4]. Experimentally, Hadzibabic *et al.* [5] had observed the interference from 30 independent condensates and obtained the surprisingly high average fringe contrast of 34%, which was indeed comparable to the results observed in the early two-condensates interference experiment of [1]. The experimental result of Hadzibabic *et al.* was in agreement with a Monte Carlo simulation.

Here, we experimentally investigate the interference of a variable number of randomly phased atomic sources. To verify the predicted $1/\sqrt{N}$ scaling of the fringe visibility as a function of the number N of sources, an array of magnetic field-insensitive ($m_F=0$) Bose-Einstein condensates is created by all optical cooling and trapping techniques. In the sites of a one-dimensional mesoscopic optical lattice potential, rubidium atoms are independently cooled evaporatively to quantum degeneracy. After releasing the microcondensates, an interference pattern is created. The observed average fringe visibility decreases with the number of coherent sources over which the atoms are distributed. Our results follow well the predictions of an exact theoretical model based on a random walk in the complex plane. In the limit of large number of condensates N, the expected $1/\sqrt{N}$ scaling of the average fringe visibility characteristic for the central limit result of the random walk is experimentally reproduced.

The observed variation of fringe visibility with the number of sources can be understood intuitively as follows. When two independent condensates with equal number of atoms are overlapped, upon measurement the condensates are projected onto a state with well-defined relative phase. This phase is random in each realization of the experiment, but in all cases a density modulation with 100% contrast occurs [7–9]. For three interfering condensates two relative phases now come into play, and in general the phase difference between any two of the condensates differs from that between either one of them and the third condensate. One still expects a periodic density modulation, but with reduced contrast. For a larger number of independent sources, the degree of randomness increases. The fringe contrast for an array of N coherent sources can be calculated with a random-walk model in which the number of steps equals the number independent phases, i.e., $N-1$ [3].

We wish to point out that the predicted $1/\sqrt{N}$ scaling of the fringe visibility with the number of sources N in the lattice is actually a far more general result when considering the degree of coherence of atomic ensembles. As a textbooklike example, let us consider a sample with N-independent monochomatic sources (single atoms in a classical model or independent condensates) with total wave function $\Phi(\mathbf{x}) \propto \Sigma_{n=1}^{N} e^{i(\mathbf{k}\cdot\mathbf{x}+\theta_n)}$, where the phases θ_n ($n=1,\ldots,N$) are randomly distributed. To test for the coherence of this ensemble, we shall beat the sample with a coherent local oscillator wave (e.g., an atom laser) with wave function $\Phi_{\mathrm{lo}}(\mathbf{x}) \propto e^{i\mathbf{k}_{\mathrm{lo}}\cdot\mathbf{x}}$. This yields a spatial interference signal $|\Phi+\Phi_{\mathrm{lo}}|^2$ with intensity modulation: $\Phi_{\mathrm{lo}}^{*}\Phi+\mathrm{c.c.} = 2\,\mathrm{Re}(e^{i(\mathbf{k}-\mathbf{k}_{\mathrm{lo}})\cdot\mathbf{x}}\Sigma_{n=1}^{N} e^{i\theta_n})$. After evaluating the average value of this random walk problem with N steps, one finds that the modulation of the fringe signal scales as $\sqrt{N}$, which compares to the value of N that is obtained with a coherent atomic ensemble. The visibility of the interference signal, a quantity commonly used when quantifying coherence in the optics literature [6], decays with a $1/\sqrt{N}$ scaling law, i.e., relatively slowly with the number of sources.

In our experimental approach, atoms are evaporated to quantum degeneracy in the sites of a one-dimensional periodic potential created by an optical standing wave generated by a CO_2 laser whose wavelength is near 10.6 μm. This laser frequency is roughly a factor of 14 below the lowest electronic resonance frequency of the rubidium atoms used in our experiment. Due to the static atomic polarizability, atoms are pulled into the antinodes of the standing wave. Adjacent sites are spaced by $d=\lambda_{CO_2}/2 \simeq 5.3$ μm, which is sufficiently far apart that tunneling between sites is completely negligible. A variable number of sites is initially occupied with thermal atoms, which are subsequently cooled to quantum degeneracy by direct evaporation in the optical trap. Our experiment benefits from recent developments in the

"all-optical" generation of Bose-Einstein condensates in optical dipole potentials [10–13], which we extend here to a lattice geometry. Besides offering the flexibility to directly evaporate into the periodic atom potential, in such traps magnetic-field insensitive condensates can be produced [12,13], which is a clear benefit in studies of coherence properties.

Let us theoretically discuss the expected interference signal after releasing the array of N (with N variable) independent microcondensates in the far field. This treatment is inspired by earlier calculations considering the interference of independent optical [14] and atomic [3,5] sources. In our model, we consider the N-independent atomic Bose-Einstein condensates with the same trap parameters in all sites before the free expansion. The total wave function at this time can be written as

$$\Phi(x) = \sum_{n=1}^{N} a_n e^{i\theta_n} e^{-(x-x_n)^2/(2l^2)}, \tag{1}$$

where $a_n e^{i\theta_n}$ denotes the amplitude of the nth condensate wave function, which is assumed to be a Gaussian function with ground-state size $l=\sqrt{\hbar/(m\omega)}$. The microcondensates are centered at the CO_2-laser lattice antinodes, corresponding to the positions $x_n=nd$, where $n=1,\ldots,N$. Because the microcondensates are independent, the phase factors θ_n are randomly distributed [7–9]. We can immediately derive the wave function in a momentum space picture $\tilde{\Phi}(p)$ by performing a Fourier transform. When expanding the atomic clouds and recording the interference pattern with a time-of-flight measurement in the far field, we actually perform a measurement of $|\tilde{\Phi}(p)|^2$, which can be written as

$$|\tilde{\Phi}(p)|^2 = \frac{l^2}{\hbar}\left[\sum_{n=1}^{N-1} A_n \cos(ndp/\hbar + \varphi_n)\right] e^{-p^2 l^2/\hbar^2}. \tag{2}$$

In this equation, $A_0=Na^2$, $\varphi_0=0$. For n other than zero, the (real) amplitudes A_n and the corresponding phase angles φ_n are given by [3] $A_n e^{i\varphi_n}=2a^2\Sigma_{q=1}^{N-n} e^{i(\theta_q-\theta_{q+n})}$, if, for the sake of simplicity, we assume equal atom population for all sites (i.e., $a_n=a$ for all n).

In our experiment, we only spatially resolve the fringe pattern with largest spatial modulation, i.e., the interference between nearest neighbors. The expected visibility of this modulation is given by $V\equiv(I_{\max}-I_{\min})/(I_{\max}+I_{\min})=A_1/A_0$, which we can write more simply as $V=2S/N$, where $S=|z|=|\Sigma_{q=1}^{N-1} z_q|=|\Sigma_{q=1}^{N-1} e^{i\Delta\theta_q}|$ and $\varphi_1\equiv\varphi$ equals the phase angle of this sum. The phase angles $\Delta\theta_q$ are randomly distributed in the range $0\leqslant\Delta\theta_q<2\pi$. For each realization of the experiment, the fringe contrast is determined by the modulus of a sum of unit vectors z_q which have random directions in the complex plane. Further, the phase angle of the total vector gives the position of the fringe pattern. In our model, the problem of calculating the fringe contrast and position of an array of coherent, independent sources thus can be transferred to the solving of a random-walk problem in the complex plane. This is a typical two-dimensional Pearson's random walk [15,16]. Figure 1(a) gives a graphical representation of the situation. In general, the expected probability density to arrive at a distance S from the origin is given by Kluyver's formula [17]

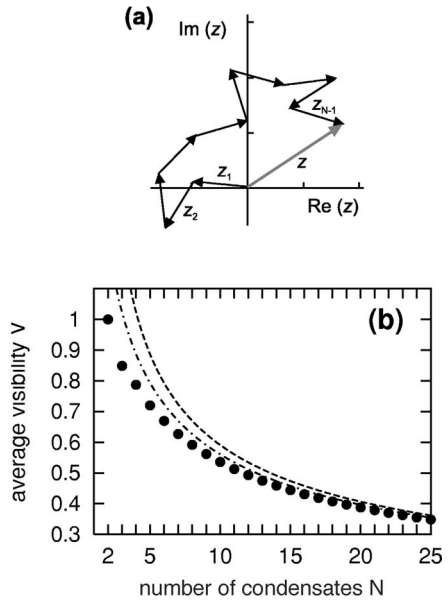

FIG. 1. (a) Random walk of coefficients $z_q=e^{i\Delta\theta_q}$, with the phase angles $0\leqslant\Delta\theta_q<2\pi$ arbitrary in the complex plane. The vector z is the sum of $N-1$ independent coefficients z_q $(1\leqslant q\leqslant N-1)$ and determines both the fringe visibility $V=2S/N$ with $S=|z|$ and its phase angle φ. (b) Predicted average fringe visibility for the far-field interference pattern of N coherent atomic sources (dots). Result of the central limit approximation: $V=\sqrt{\pi/(N-1)}$ (dashed line) and the simple $V=\sqrt{\pi/N}$ scaling function (dashed-dotted line).

$$p(S,N-1) = \frac{1}{N-1}\int_0^\infty [J_0(\rho)]^{N-1} J_0(S\rho)\rho d\rho, \tag{3}$$

where J_0 is the zeroth Bessel function. For large N, the Bessel functions can be asymptotically expanded, and a Gaussian probability distribution is obtained, corresponding to the celebrated central limit result [16]. In this approximation, the expected average visibility approaches the previously derived value of $\sqrt{\pi/(N-1)}\simeq\sqrt{\pi/N}$, when $N\gg1$ [3]. Note that $N-1$ equals the number of relative phases between adjacent sites and therefore the number of steps of the random walk. In the general case, and especially for a small number of condensates, one has to fully solve Eq. (3), which is difficult due to the oscillatory character of the Bessel functions. We have numerically evaluated the probability density by expanding Kluyver's formula in a Bessel-Fourier series [14]. As an independent verification of our calculation, we performed a Monte Carlo analysis of the average visibility assigning random values to the arguments $\Delta\theta_q$. Figure 1(b) shows the theoretical expected fringe average visibility as a function of condensate number derived using the exact calculation (dots), the central limit result (dashed line), and the simple $\sqrt{\pi/N}$ scaling function (dashed-dotted line).

An array of independent Bose-Einstein condensates with variable number of sites is produced using a modification of our previous setup [13,18]. In an ultrahigh vacuum chamber, midinfrared radiation near 10.6 μm for atom trapping is focused to a beam waist ($1/e^2$ radius) in the range 25–40 μm. With a second lens and a retroreflection mirror, a standing wave is generated. The size of the beam waist in the trapping

region could be varied with a telescope. This gave us control over the number of populated trapping sites. For a loading of atoms, we switched to a running wave geometry by slightly misadjusting the CO_2-laser beam backreflection mirror away from a perfect retroreflection. This mirror was mounted on a piezo, which allowed for an electronic control of the degree of alignment during the course of the experiment. Cold rubidium (^{87}Rb) atoms from a magneto-optical trap (MOT) were loaded into the running wave geometry. After this transfer, 10^6 atoms, populating the lower hyperfine ground state ($F=1$, $m_F=0,\pm1$) are left in the optical trap at a temperature near 100 μK. To cool the trapped atomic cloud, the CO_2-laser beam power is acousto-optically ramped down to induce forced evaporative cooling. The highest energetic atoms leave the purely optical trap, and the remaining ones thermalize to lower temperatures. The total evaporation stage lasts about 10 s, during which the midinfrared beam power is smoothly reduced from 30 W to a typical final value of 40–50 mW. Throughout the evaporation stage, the MOT quadrupole field with 10 G/cm field gradient is left on. This gradient is sufficiently strong to remove atoms in field-sensitive spin projections in this running wave geometry, as the trapping force along the beam axis is here relatively weak [19]. While the initial phase of this evaporation is still performed in the running wave geometry (this limits the number of sites over which atoms are distributed), during the course of the evaporative cooling we slowly switch to a standing wave (lattice) geometry by servoing the piezo-mounted mirror correspondingly. The 1D lattice geometry is fully aligned at a time 1–2 s before the onset of quantum degeneracy (corresponding to atomic temperatures a factor of 2 above the transition temperature of about $T_c \simeq 200$ nK). This ensures that the microcondensates are formed independently.

At the end of the evaporation state, an array of $m_F=0$ microcondensates is created. The total number of atoms in the optical lattice is about 7000, and the number of condensed lattice sites can be varied from typically 5 to 35 by choosing different beam waists of the lattice beams and—in a smaller range—also allowing for tiny residual misalignments of the lattice beams at given beam diameter. For all our measurements, the estimated tunneling time between sites is above 10^{18} s. This assures that the microcondensates are truly independent. The residual sensitivity of the $m_F=0$ condensates to stray magnetic fields due to the second-order Doppler shift is near 14 fK/mG^2. For a typical extension of the lattice of 100 μm, the variation of the condensate phases due to magnetic field inhomogeneities is 0.15 Hz at an estimated field gradient of 50 mG/cm. On the other hand, we expect that differential mean-field shifts due to variation in the atom number do cause a non-negligible differential variation of the condensate phase with time.

After creation of a variable number of microcondensates in the lattice, the CO_2-laser radiation is extinguished, and the atomic clouds are allowed to freely expand and fall in the earth's gravitational field. The atomic distribution recorded to a time of flight of 0 ms was well described by a spatially constant function with smooth edges. This allowed us to assume equal population in the lattice region. The condensed atomic clouds originating from adjacent sites overlap as soon as the free expansion time t exceeds 0.5–1.5 ms, depending

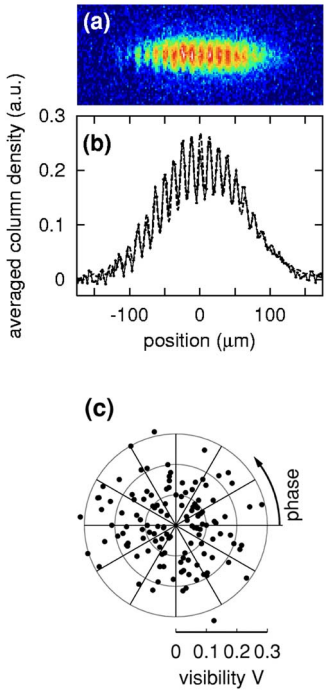

FIG. 2. (Color online) (a) False-color absorption image of an interference pattern of 20 independently generated $m_F=0$ microcondensates released from a CO_2-laser optical lattice. The image was recorded after a free expansion time of 15 ms. The field of view is 350×140 μm. (b) Horizontal profile of the image averaged over a vertical region of 35 μm: Experimental data (solid line with dots) and fitted fringe pattern (dashed line). (c) The fringe visibilities and phase angles of fringe patterns arising from the interference of 20 independent Bose-Einstein condensates, derived from fits as in (b), have been drawn (dots) in a polar diagram for 130 different realizations of the experiment.

on the interaction energy for the particular atom population per site, which in turn depends on N. We then expect to observe an interference pattern with spatial period of $\lambda_{\mathrm{th}} = ht/(md)$, despite each individual atom source having random phase. Figure 2(a) shows a typical observed interference pattern for $N=20$ interfering coherent atomic clouds. The free expansion time here was $t=15$ ms, after which the shown absorption image was recorded. A horizontal profile of this image is shown in Fig. 2(b), where the dashed line with dots shows the experimental data. For an analysis of our data, the fringe patterns (i.e., the absorption image profiles) were fitted with the function

$$I(x) = I_0[e^{-(x-x_0)^2/\sigma^2} + V_{\mathrm{expt}}e^{-(x-x_0')^2/\sigma'^2} \times \cos(2\pi x/\lambda_{\mathrm{expt}} + \varphi_{\mathrm{expt}})], \quad (4)$$

where λ_{expt} and φ_{expt} denote the fitted fringe spacing and the phase angle of the interference pattern, respectively. Gaussian envelopes with independent widths and positions are included here for the background and fringe signals, respectively. The fringe visibility V_{expt} of the pattern of Fig. 2(a), as derived from the fit, was 31.5%. The experimental fringe spacing here is $\lambda_{\mathrm{expt}} \simeq 13.0\pm0.3$ μm, which agrees well with the expected spacing $\lambda_{\mathrm{th}} \simeq 12.97$ μm. We have studied the variation of fringe contrast and phase angle for different re-

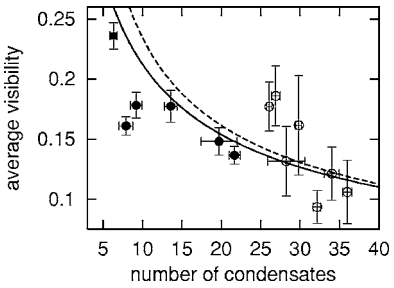

FIG. 3. Average fringe visibilities of far-field interference patterns as a function of number of interfering coherent atomic sources. The experimental data sets were recorded with beam waists: 24.3 μm (squares), 30.0 μm (dots), and 40.2 μm (circles). The data have been fitted with the (interpolated) theoretical fringe contrast multiplied by a constant factor, which is left as a free parameter to account for the finite imaging resolution (solid line). The dashed line gives the corresponding result in the central limit approximation when assuming the same imaging resolution.

alizations of the experiment. Figure 2(c) shows these parameters in a polar plot, where each dot corresponds to the result of an individual realization. Phase angles and fringe contrasts here vary randomly from measurement to measurement. Moreover, no preference for a certain value of phase angle is visible. Note the close analogy of this polar image to Fig. 1(a). The vector $z=Se^{i\varphi}$ as a complex signal modulation [where $S=(N/2)V$] represents the endpoint of a random walk in the complex plane, and can be directly determined experimentally from fringe contrast and phase of a far-field interference pattern. Series of fringe patterns were recorded for different numbers N of populated lattice sites.

Figure 3 shows the variation of the average fringe visibility for a series of measurement as a function of N. The (average) number of populated sites here was determined by recording the length of the lattice, as measured with a time-of-flight image at zero expansion time [20]. Our experimental data clearly show a decrease of the fringe contrast with condensate number, which agrees with the exact random-walk solution valid for arbitrary N [see Eq. (3)] and within our experimental uncertainties also with the central limit result. For large number of independent sources, the fringe contrast averages out. However, this averaging effect occurs relatively slowly, i.e., it takes a large number of sources to let the fringe pattern resemble that of an incoherent atomic sample. The data shown in Fig. 3 have been fitted with the (interpolated) result of the exact random-walk calculation for a lattice with equally populated sites, as shown by the solid line. To account for our experimental imaging resolution, we have multiplied the theoretical result with a constant value, which was the only free parameter in the fit. The resolution of 6.3 μm obtained in this way agrees well with an independent, direct measure of the optical resolution of 6.0 μm. The dashed line gives the corresponding visibilities using the simple $\sqrt{\pi/(N-1)}$ result of the central limit approximation, which was multiplied with the same constant factor.

To conclude, we have studied the interference of an array of independently generated $m_F=0$ microcondensates in an optical lattice for a variable number N of populated sites. The observed average interference visibility decreases with source number due to the increased number of (upon measurement) randomly distributed relative phases, and follows well the predicted $1/\sqrt{N}$ scaling.

For the future, we anticipate that the observed relatively slow decay of coherence with source number will allow one to observe related interference effects with small samples of thermal atoms. A further direction for future research would be to experimentally verify the intrinsic (i.e., quantum-mechanical) randomness of the relative phases of the atom sources. Due to the use of $m_F=0$ condensates, differential phase shifts due to stray magnetic fields are estimated to contribute clearly below a radian. In our current experiment, differential mean-field phase shifts due to the (in general) slightly different atom numbers per site during the approximately 1–2 s time period between the onset of quantum degeneracy and the release of the microcondensates, are however estimated to still accumulate statistical variations of the phase φ of several tens of radians from shot to shot. If, e.g., measurements with constant atom number per site could be postselected, which clearly requires small absolute atom numbers, the intrinsic randomness of the condensates relative phase might be experimentally tested. Finally, we anticipate that our experimental scheme holds promise for certain types of lattice atom lasers.

We acknowledge financial support from the Deutsche Forschungsgemeinschaft, the Landesstiftung Baden Württemberg, and the European Community.

[1] M. R. Andrews *et al.*, Science **275**, 637 (1997).
[2] See, e.g., I. Bloch, Phys. World **17**, 25 (2004).
[3] S. Ashhab, Phys. Rev. A **71**, 063602 (2005).
[4] A. R. Kolovsky, Europhys. Lett. **68**, 330 (2004); R. Bach and K. Rzazewski, Phys. Rev. A **70** 063622 (2004).
[5] Z. Hadzibabic *et al.*, Phys. Rev. Lett. **93**, 180403 (2004).
[6] See, e.g., E. G. Steward, *Fourier Optics* (Ellis Horwood, Chichester, 1989).
[7] J. Javanainen and S. M. Yoo, Phys. Rev. Lett. **76**, 161 (1996).
[8] M. Naraschewski *et al.*, Phys. Rev. A **54**, 2185 (1996).
[9] Y. Castin and J. Dalibard, Phys. Rev. A **55**, 4330 (1997).
[10] M. Barrett *et al.*, Phys. Rev. Lett. **87**, 010404 (2001).
[11] T. Weber *et al.*, Science **299**, 232 (2003).
[12] Y. Takasu *et al.*, Phys. Rev. Lett. **91**, 040404 (2003).
[13] G. Cennini *et al.*, Phys. Rev. Lett. **91**, 240408 (2003).
[14] See e.g., E. Merzbacher *et al.*, Am. J. Phys. **45**, 964 (1977).
[15] K. Pearson, Nature (London) **LXXII**, 294 (1905).
[16] See e.g., G. H. Weiss, *Aspects and Application Of The Random Walk* (North-Holland, Amsterdam, 1994).
[17] J. C. Kluyver, Konink. Acad. Wetenschap te Amst. **14**, 325 (1906).
[18] G. Cennini *et al.*, Appl. Phys. B: Lasers Opt. **77**, 773 (2003).
[19] The center of the MOT quadrupole field is in general not perfectly aligned with the optical dipole trap.
[20] Experimentally, the lattice site population along the beam axis resembled a top hat function with soft edges.